

Heavy metal ions removal from oil wastewater using highly enhanced Chitosan membrane technology: a response surface methodology study

Wato N. Fundji, Ephraim Igberase*, Peter O. Osifo, John Kabuba

Department of Chemical Engineering, Vaal University of Technology, South Africa

*Corresponding author E-mail: ephraimig@vut.ac.za

Article info

Received 17/12/2022; received in revised form 22/12/2022; accepted 30/12/2022

DOI: [10.6092/issn.2281-4485/16047](https://doi.org/10.6092/issn.2281-4485/16047)

© 2022 The Authors.

Abstract

This paper investigates the removal of heavy metal ions from oily wastewater using enhanced Chitosan Membrane. Cellulose and gelatin have been used successfully to modify chitosan. Fourier Transform Infrared (FTIR), Scanning Electron Microscopy (SEM), and X - Ray Diffraction (XRD) were used to characterize chitosan. We looked at the impacts of pH solution and conductivity. To eliminate the heavy metals, adsorption study was conducted. Results showed removal percentages higher than 90% especially when the initial pH is 7.50 and the volume of Hexane is 12 mL. Conductivities of wastewater were positive and negative depending on whether the medium is acidic and basic respectively and values higher than +260 mV and lower than -340 mV were observed. Experiments were designed employing Central Composite Design (CCD) of the Response Surface Methodology to examine the effects of experimental conditions (RSM). R^2 values for analysis of variances of Cu^{2+} , Fe^{2+} , and Pb^{2+} were all almost the same at 0.99. The quadratic models appeared significant and adequate in evaluating the experimental results. The differences in experimental and projected % Removal values were negligible for all models. The 3D response surface plots that resulted permitted paired analysis of variable impacts on each response model.

Keywords

Chitosan, Membrane, Removal, pH

Introduction

Oil is one of the key sources of energy for people living in developed nations. In the course of the oil phase (for discovery, regular transportation, treatment, dumping, and run-offs from industry), the accidental leakage of oils to a marine environment in the form of recurrent oil spills also poses a major global problem (Islam, 2015; Doshi *et al.*, 2017; Khalifa *et al.*, 2019; Marafi *et al.*, 2019; Wolok *et al.*, 2020) low-cost oil adsorptive materials based on chitosan (CS). Existing literature has shown that various offshore oil zones are also polluted with heavy metals, which serve as an obstacle for native

biodiversity. The co-contamination of petroleum with trace metals is most frequent in oil spill sites (Islam, 2015; Tiwari *et al.*, 2017). It is critical to eliminate ions of heavy metals from wastewater. Organic solvents employed mostly in the interfacial polymerization, such as benzene, dichloromethane, heptane, cyclohexane and n-hexane are often carcinogenic, teratogenic, and mutagenic (Ma *et al.*, 2022). Metal salts and organic linkers are combined in the liquid phase, with or without the assistance of auxiliary molecules. The careful selection of reaction solvents is critical since they directly or indirectly impact metal coordination behaviour. Although the reason for the solvent selection

for each synthesis is yet unknown, each solvent system plays a role in controlling the creation of distinct coordination environments. The solvents utilized in the process can either engage in metal ion coordination or function as a guest molecule inside this even-tual crystalline lattice (Seetharaj *et al.*, 2019). According to Rayhani, Simjoo and Chahardowli (2022), the petroleum polar components, such as asphaltene, resins, and fatty acids, operate as surface-active agents at the oil-water interface, promoting the development of in situ Water/Oil emulsification. Machine oil is converted throughout usage owing to the dissolution of additives, contaminants with combustion products, and the build-up of metals such as Magnesium, Copper, Zinc, Lead, Cadmium, and such from engine. As a result, the composition of used engine oil is hard to extra-polate or define in precise chemical terminology (Adeleye *et al.*, 2018). A range of processes is reported for cleaning polluted wastewater and other wastewaters. Advanced eco-friendly equipment to remove leaked oil are urgently needed (Wolok *et al.*, 2020). For this reason, various technology and procedures are currently used. Chemisorption, ion exchange, physisorption, and membrane technology are all com-mon techniques for removing metal ions from waste-water. Among these technologies, membrane separa-tion is regarded the most promising because of its ease of use, high separation efficiency, lack of secondary contamination, and ease of recovery of separated products. To begin, the porous support is submerged during an amine-containing aqueous stage. To gene-rate the Polyamide layer, the acid chloride is dissolved in the organic solvent and then poured onto the soaked support. Polysaccharides have recently become very interesting as scaffold products, because their moistens of carbohydrates associate with or shape an essential part of several cell adhesion molecules and glycoprotein matrix (Chiono *et al.*, 2008). As pure and organic raw material with ample supplies and no emissions, polysaccharides have a high temperature and shear tolerance (Chen *et al.*, 2020). Chitosan has been particularly important here because it can be used in the treatment of aqueous effluents among its numerous applications (Da Silva Grem *et al.*, 2013). Chitosan, an N-deacetylated polysaccharide, is the D-glucosamine and C-acetyl-D-glucosamine copolymer (Islam *et al.*, 2015; Mitura *et al.*, 2020; Omer *et al.*,

2021; Zakuwan *et al.*, 2021). To the greatest of our knowledge, no research on the removal of Cu^{2+} , Fe^{2+} , Pb^{2+} including the influence of pH, temperature, time and Hexane as variables in the process of removing heavy metals from oily wastewater employing modi-fied chitosan has been reported. The purpose of this study was to look at the influence of solution pH and Hexane. To investigate the impacts of experimental settings, experiments were constructed using Central Composite Design (CCD) based on Response Surface Methodology (RSM). The RSM's CCD was used to compute the total number of experiments conducted in the experiment, and analysis of variance was performed to evaluate the model's significance but also suitability.

Materials and Methods

Materials and preparations

Chitosan with a deacetylation level of 90% was purchased from Aldrich (USA). Analytical grade of sodium hydroxide (NaOH, purity: 98%), potassium hydroxide pellets (KOH, purity: 85%), n-Hexane ($\text{n-C}_6\text{H}_{14}$, purity: 95%), acetone [$(\text{CH}_3)_2\text{CO}$, purity: 99.5%], sulfuric acid (H_2SO_4 , purity: 98%) and glacial acetic acid (CH_3COOH , purity: 100%) were utilized. Sulfuric acid had to be diluted from initial concentration of 18.4 M to 0.01 M while 0.01 M of KOH had to be prepared for adjusting of pH. 0.01 M of NaOH was prepared and was used when testing the synthesized membrane. Acetic acid was also diluted from original concentration of 17.5 M to 1 M and was the solvent used as the solvent to dissolve to prepare membranes. 8 g Chitosan powder was combined with 2 g Cellulose as well as 2 g Gelatin. 500 mL of 1M acetic acid was used to dissolve the powder combination. For an hour, the aqueous solution was put on a heated plate at 250°C and stirred at 200 rpm. Water-oil solution in which the oil would be on top of the water level and is mixed thoroughly under extreme turbulence, simulating real-world environmental conditions. The hexane-water solution was forcefully agitated using a magnetic stirrer to produce this turbulent effect. Following that, the solution was removed from the hot plate and allowed to cool somewhat at ambient temperature for an hour. The gelly fluid was then spread onto plastic PVC sheets before even being dried at 30°C for 18 hours to solidify yet remain flexible. As a result, the membrane was separated from the plastic PVC sheets in order to remove heavy oil from wastewater. The samples were placed in the oven

for at least 18 hours then they were removed from it. The products were collected and the membranes were detached from the plastics as displayed in the Figure 1.

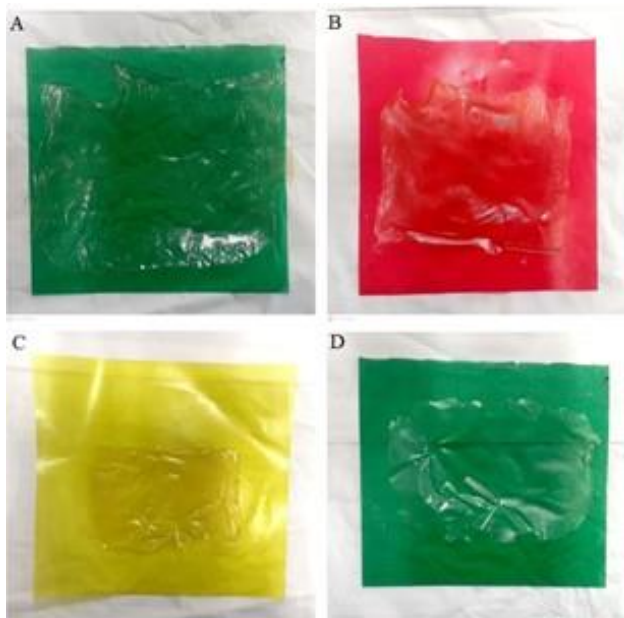


Figure 1. Membrane sample products.

The drying process has occurred in the oven at 30°C for at least 18 hours. After the drying phase, the product had to be flexible and foldable in order to be used. This happened only if the temperature in the oven was set around room temperature (De Lima *et al.*, 2009; Zakuwan *et al.*, 2021). In Figure 1, (A) was the membrane prepared only with chitosan. The membrane in (B) was the combination Chitosan – Cellulose; the one in (C) was that of Chitosan – Gelatin and (D) was the one with Chitosan – Cellulose – Gelatin.

Characterization of Membranes

Fourier Transform Infrared spectroscopy (FTIR) analysis was performed utilising Perkin Elmer spectrum FT 400 to characterize the chemical structure of chitosan, cellulose, gelatin and of the modified chitosan three operating pH mediums of the solution: 3, 7.5 and 12. Samples were labelled accordingly, and all data were established using 400–4000 cm⁻¹ range. Scanning Electron Microscopy (JEOL JSM-IT500) with a 5 – 10 kV acceleration voltage was used to explore the surface morphology of Chitosan, cellulose, gelatin, and all membranes. It was also used to determine their elemental composition A sputter coater unit applied a thin gold coating to the samples using from ×43 to ×230 magnification. X – Ray diffraction (XRD) analysis was performed using X-ray diffractometer (Smartlab 3 KW,

Rigaku Corporation, Japan) to assess the crystalline phase of chitosan, cellulose, gelatin, and membranes using Ni-filtered Cu K radiation ($\lambda = 1.54 \text{ \AA}$) generated at 40 kV and 40 mA voltage and current settings. The angle was adjusted at a steady rate throughout a 2 θ range of 0°–90°. The Quadrupole-Inductively Coupled Plasma Mass Spectrometry (QICPMS, iCAPQ thermo fisher scientific) technology was used to quantify ions contained in the oily wastewater before and after sorption with synthesized membrane of modified chitosan. Considering that C_o (mg/L) would be the original concentration of metal ions in solution and C_e (mg/L) is the concentration after filtering, the percentage removal of heavy metal ions was calculated using equation [1]:

$$\% \text{ Removal} = \frac{C_o - C_e}{C_o} \times 100 \quad [1]$$

In this study, the parameters considered were investigated using design expert version 6.0.6 software. The software analysed the responses of each through the analysis of variance (ANOVA) and 3D model graphs.

Results and Discussion

Fourier Transform Infrared Spectroscopy (FTIR) analysis

In Figure 2, the significant differences are as follows: (a) A firm absorption peak at around 1566 cm⁻¹ corresponding to the C=N stretching formed between the aldehyde and amine groups, (b) Absorption band at around 2937 for Chitosan –CH stretching, and (c) Absorption band at around 1420 cm⁻¹ for the merger between –NHCO (Amide III) band at 1395 cm⁻¹ of chitosan. In the 3100–3700 cm⁻¹ range, which marks OH groups.

The peaks at 2920 and 2960 cm⁻¹ are attributed to bending vibrations of asymmetric and symmetric CH₂ groups, correspondingly. Furthermore, the peak at 2850 cm⁻¹ is caused by the stretching vibration for –CH groups. The peaks at 1710 as well as 1650 cm⁻¹ are mainly attributed to the carbonyl groups of COOH and CONH, respectively. The stretching vibration of COH caused the distinctive peaks to arise at 1045 and 1280 cm⁻¹. The large peak at 3325 cm⁻¹ in spectra (B) is caused by hydrogen bound Hydroxyl group in cotton fabric. The peak at 1635 cm⁻¹ is caused by absorbed water molecules (Abdel-Hakim *et al.*, 2021)poly(AA-

co-NMA. Peaks in the vibrational properties of CH₂ in plane bends is distinguished by peaks at 1315 and 1200 cm⁻¹. The OH peaks were observed at 2894, 1424, and 1370 cm⁻¹. The OH peaks in plane bends is distinguished by peaks at 1315 and 1200 cm⁻¹.

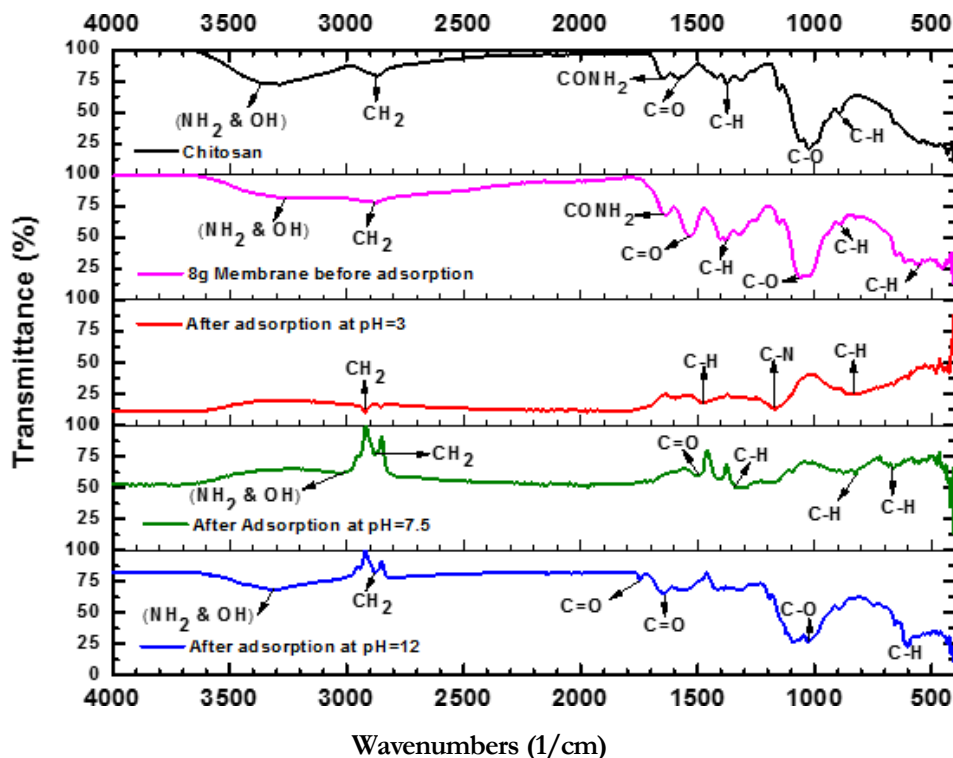


Figure 2. Changes in the Chitosan membrane

The peaks at 1156 and 1034 cm⁻¹ are caused by asymmetric bridging COC and asymmetric stretching of CO, respectively (Abdel-Hakim *et al.*, 2021) poly(AA-co-NMA. Although the solvents are not usually integrated, they do serve as a structural guiding agent or an environment for the crystal development process. In other words, the degree of deprotonation of organic carboxylate compounds may be adjusted by choosing appropriate solvents or altering the basicity of the solvent medium. At higher temperatures, these solvents can be converted to their corresponding amines, resulting in carboxylate deprotonation (Seetharaj *et al.*, 2019).

Scanning Electron Microscope (SEM) analysis

Figure 3, and the quantity of oil used throughout the current study is very negligible; and also, the SEM observations are performed on dried samples under vacuum, and dehydration of such oil - in - water is particularly prone to destroying the emulsion and fundamentally changing its surface.

Scanning Electron Microscopy was also used to investigate the topography, surfaces, structures, morpho-

logies, and composition of chitosan Nano-particles after removal and, at this point, only the ratios of 8: 2: 2 was studied as displayed in Figure 3 which showed the area of the Chitosan membranes had a porous shape. It's worth noting that the functionalized surface retains its porous shape, complete with micro-sized pores (Zhu *et al.*, 2021).

Figure 3 showed cross-sectional topologies of Chitosan membranes with almost the same three-dimensional structure and large porosity, revealing that surface functionalization happened solely on the surface. It has been found that separation polymers with high adsorption capacity and high porosity can give excellent oil/water removal efficiency (Zhu *et al.*, 2021).

The chitosan surface was already rougher. It was remained rough after alteration, but with more irregularly shaped particles, which was linked to the breakage of hydrogen bonding, resulting in microfibrils (Yu *et al.*, 2020). After removing the oils, uneven triangular shapes on the surface of membranes were detected in Figure 3. Despite the fact that the roughness was fading, the presence of oil began to affect the surface properties (Yu *et al.*, 2020).

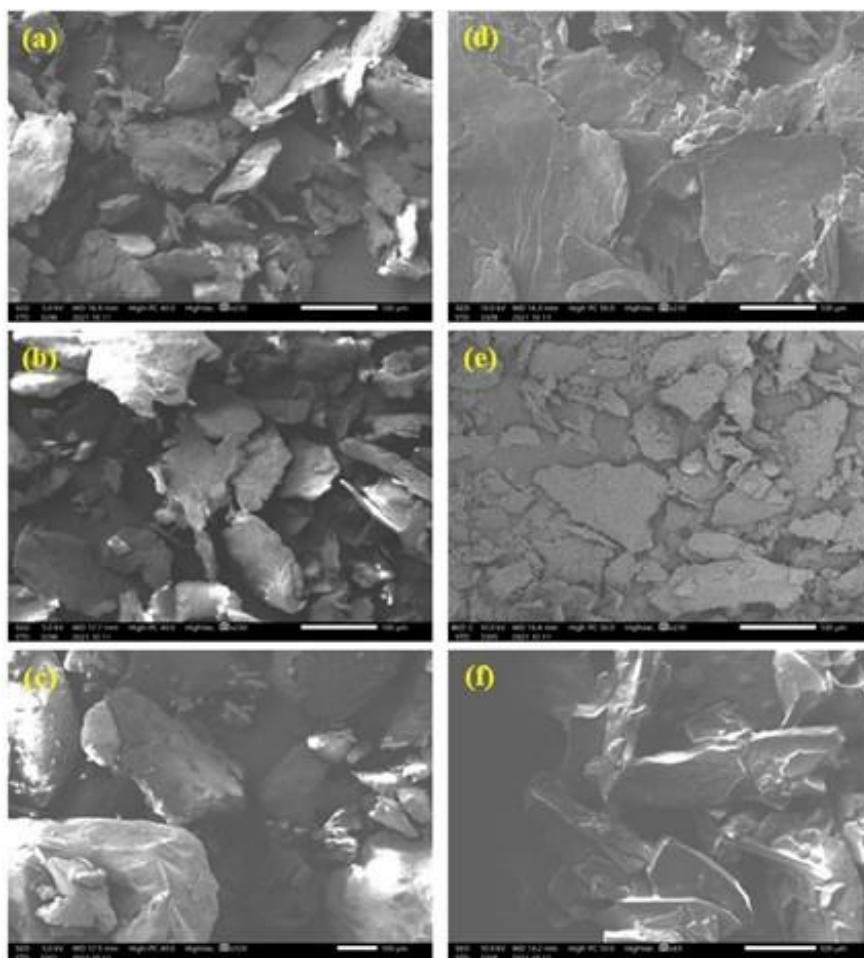


Figure 3. SEM of chitosan (a), cellulose (b), gelatin (c), membranes after removal at pH = 3 (d), pH = 7.5 (e) and pH = 12 (f)

X – Ray Diffraction analysis (XRD)

In Figure 4, the XRD results of chitosan was compared with four products: the membranes made from 8g chitosan alone, 8 g chitosan with 2 g cellulose, 8 g chitosan with 2 g gelatin and 8 g chitosan with both 2 g cellulose and 2 g gelatin as required in this study. From all those patterns, only the powder of chitosan presented a peak at $2\theta = 20^\circ$. There were different peaks in Figure 4 for the prepared membranes due to the modification of chitosan: one at $2\theta = 22^\circ$, then at $2\theta = 21^\circ$, another one at $2\theta = 21^\circ$, and also at $2\theta = 22^\circ$ respectively for the chitosan alone, chitosan/cellulose, chitosan/gelatin and chitosan/cellulose/gelatin combinations.

All the peaks in Figure 4 were due to crystal in the chitosan structure, and they had been present due to high degree of crystallinity as reported by Fathy, Selim and Shahawy (2020) Fourier transform infrared spectroscopy (FT-IR and the shifts also occurred due to

chitosan modification. Chitosan profiles revealed a peak at 2θ , which matched to 110 reflections, indicating a typical x-ray diffraction pattern. However, in chitosan XRD profiles, the peaks fell dramatically and were replaced by a dispersive wide peak, indicating a loss in crystallinity (Wang *et al.*, 2016). The loss of crystallinity suggested that the change of the chitosan backbone impaired the chitosan's hydrogen bonding capacity and disrupted the original structure of chitosan (Wang *et al.*, 2016). The reaction medium's acidity/basicity is commonly acknowledged to have a significant influence on the crystallization and evolution of inorganic-organic biomaterials. The likelihood of crystallization is increased due to the high solubility of the reactants, and big crystals of excellent quality are formed in hydrothermal synthesis. When the ligands utilized are not entirely soluble under normal circumstances, hydrothermal synthesis is also required (Seetharaj *et al.*, 2019).

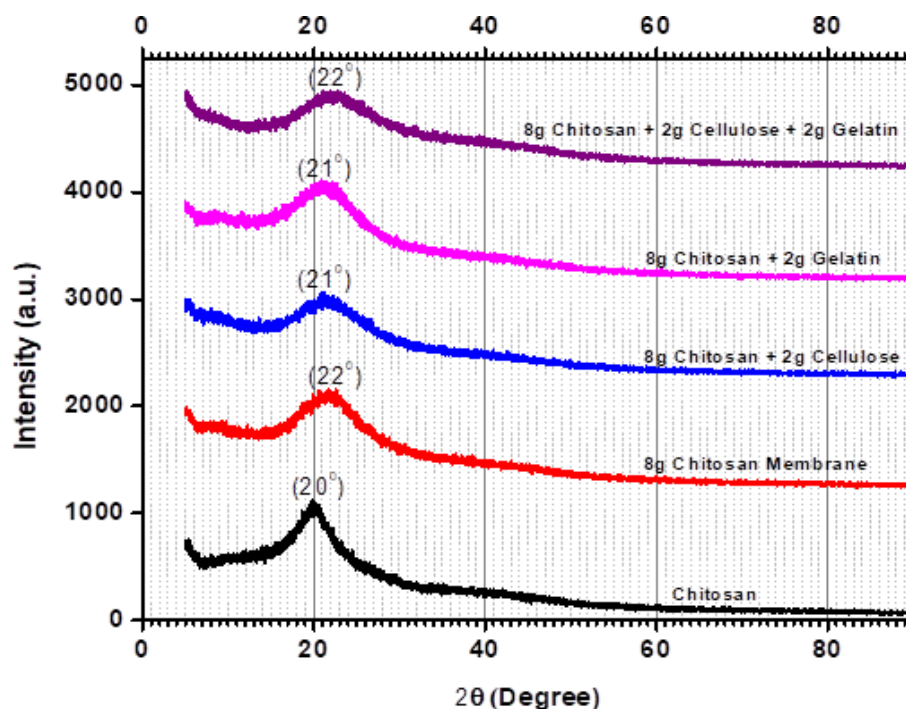


Figure 4.
XRD of the
modification of
Chitosan.

Elemental composition of Materials and Membranes

Composition of materials and Membranes before removal. The composition of Chitosan, cellulose and gelatin, as shown in Table 1, revealed that these compounds had been organic just as reported many authors (Da Silva Grem *et al.*, 2013; Khalifa *et al.*, 2019; Lakra, Balakrishnan and Basu, 2021, etc. causing serious damages. Among various treatment methods, adsorption is generally considered the most appropriate, since it can remove both organic and inorganic pollutants. Adsorption using low-cost alternative biopolymers for removal of contaminants from wastewater has been widely investigated. In this context, chitosan has been drawing particular attention because, among its many

applications, it can be used in the treatment of aqueous effluents. In this study, microspheres were prepared by reticulation of chitosan with sodium triphosphate (STP). The existence of carbon and oxygen stood out the most in the findings of this study. However, additional elements like as hydrogen and nitrogen are not excluded. These final two were found to be present during characterisation in the FTIR data in this study. Before oil removal, chitosan, cellulose, gelatin, and all membranes had a tendency for their carbon mass percent to always be larger than their oxygen and nitrogen mass percent. Many writers have already stated in the literature that chitosan, cellulose, and gelatin were truly lengthy organic chains.

Table 1. Elemental composition of materials and membranes before removal

Elements	Materials composition (wt %)		
	Chitosan	Cellulose	Gelatin
C	56.95 ± 0.66	50.46 ± 0.60	64.09 ± 0.65
O	43.05 ± 1.29	41.64 ± 1.24	35.91 ± 1.12
N	---	7.90 ± 0.66	---

Modification with combinations of 8 g Chitosan (wt.%)				
Elements	8 g Chitosan only	8 g Chitosan - 2 g Cellulose	8 g Chitosan - 2 g Gelatin	8 g Chitosan - 2 g Cellulose - 2 g Gelatine
C	51.58 ± 0.90	50.95 ± 0.97	60.07 ± 1.21	52.45 ± 1.14
O	48.42 ± 2.00	49.05 ± 2.16	39.93 ± 2.61	47.55 ± 2.51
N	---	---	---	---
Modification with combinations of 10 g Chitosan (wt.%)				
Elements	10 g Chitosan only	10 g Chitosan - 2 g Cellulose	10 g Chitosan - 2 g Gelatin	10 g Chitosan - 2 g Cellulose - 2 g Gelatine
C	54.27 ± 0.38	61.57 ± 0.59	53.00 ± 0.87	50.68 ± 0.98
O	45.73 ± 0.41	38.43 ± 1.17	47.00 ± 1.91	49.32 ± 2.21
N	---	---	---	---
Modification with combinations of 12 g Chitosan (wt.%)				
Elements	12 g Chitosan only	12 g Chitosan - 2 g Cellulose	12 g Chitosan - 2 g Gelatin	12 g Chitosan - 2 g Cellulose - 2 g Gelatine
C	50.88 ± 0.69	58.99 ± 0.77	59.61 ± 0.73	56.77 ± 0.76
O	49.12 ± 1.55	41.01 ± 1.56	40.39 ± 1.48	43.23 ± 1.59
N	---	---	---	---

Changes in the composition of membranes after removal. Table 2 showed organic contents of membranes (12: 2: 2 and 8: 2: 2 ratios) after removal of oil. Results

showed the appearance of potassium (K). This was due to the use of potassium hydroxide while adjusting the pH especially when operating under pH 12.

Table 2. Elemental composition of membranes after removal

Elements	Membrane changes (8: 2: 2 mass ratio)			
	Initial Membrane	pH 3	pH 7.5	pH 12
C	52.45 ± 1.14	85.21 ± 0.84	51.94 ± 0.63	78.83 ± 0.76
O	47.55 ± 2.51	14.79 ± 1.06	40.25 ± 1.39	20.62 ± 1.12
N	-	-	7.81 ± 1.00	0.01 ± 0.58
K	-	-	-	0.55 ± 0.33
Elements ratio)	Membrane changes (12: 2: 2 mass			
	Initial Membrane	pH 3	pH 7.5	pH 12
C	56.77 ± 0.76	31.20 ± 1.68	65.10 ± 0.62	55.81 ± 0.65
O	43.23 ± 1.59	67.15 ± 5.11	30.91 ± 1.01	32.32 ± 1.30
N	-	1.65 ± 1.28	3.99 ± 0.49	-
K	-	-	-	11.87 ± 1.07

Permeability of Membrane

The inherent permeation of modified membranes had been evaluated utilizing water filter as reported by Zhao *et al.* (2021) conventional membranes usually suffer from severe pore clogging and surface fouling, and thus, novel membranes with superior wettability and

antifouling features are urgently required. Herein, we report a facile green approach for the development of an underwater superoleophobic microfiltration membrane via one-step oxidant-induced ultrafast co-deposition of naturally available catechol/chitosan on a porous polyvinylidene fluoride (PVDF).

Composition	% Recovery of distilled water volume			Table 3. Water recovery: capacity comparison
	NaOH spread on membrane	KOH spread on membrane	H ₂ SO ₄ spread on membrane	
Chitosan only	45	45	65	
Chitosan–Cellulose	70	65	70	
Chitosan–Gelatin	80	85	85	
Chitosan–Cellulose–Gelatin	55	70	75	

The findings in the Table 3 compared different volumes recovered from the initial capacity of distilled water, depending on compositions and chemicals spread on the surface of the membrane. The very same patterns to modified chitosan had been used to evaluate the water recovery capacity. Results showed the good effect of modifying chitosan with cellulose and gelatin. The chemicals spread on the membranes also had an impact on them in the recovery of the fluid. Spreading of those chemicals was done before putting the gelly samples into the oven at 30°C for 18 hours in order to dry the samples and to obtain membranes. The lowest recovery percent (45%) was obtained while spreading sodium hydroxide. That was because chitosan had not yet been modified. But still, it showed that chitosan membrane alone could also be permeable as reported in the Literature by many authors (De Lima *et al.*, 2009;

Sakwanichol, Sungthongjeen and Puttipipatkachorn, 2019; Mruthunjayappa *et al.*, 2020). The modification of chitosan with cellulose and gelatin had improved the recovery capacity from 45 to 55% while using sodium hydroxide, from 45 to 70% while using potassium hydroxide and from 65 to 75% when using sulfuric acid. Crosslinking with sulfuric acid had been the main reason why the recovery capacity was higher compared to the sodium hydroxide and the potassium hydroxide as Fideles *et al.* (2018) reported that Crosslinks have been generated after evaporation of the solvent on chitosan membranes as well as a treatment with sulfuric acid solution. The presence also of gelatin in the membrane had increased the recovery according to the findings in Table 4. This was due to the porosity of the gelatin reported by Deshmukh *et al.* (2017)

Composition	Volume recovered (mL) / 20 mL distilled water volume			Table 4. Water recovery: pH comparison
	Recovery volume in %	pH before removal	pH after removal	
Chitosan only	60.30	8.47	7.93	
Chitosan–Cellulose	70.30	8.47	7.85	
Chitosan–Gelatin	80.30	8.47	7.93	
Chitosan–Cellulose–Gelatin	75.30	8.47	7.92	

Findings in Table 4 showed the recovery volume percent and the variation in pH of the treated samples. Although membranes with chitosan alone had the lowest recovery percent compared to the three other combinations, results had once again supported the permeability of chitosan (De Lima *et al.*, 2009; Sakwanichol, Sungthongjeen and Puttipipatkachorn, 2019). Samples of oily wastewater were synthesised, and its pH were measured to make them pass through four different membranes respectively to the same combinations in Table 4 and their pH after the passage was decreased compared to the initial wastewater sample.

Changes in parameters before and after removal: pH, Conductivity

Table 5 also included the findings that were taken into account while creating the chemically synthesized solution for the response surface approach. Experiments were carried out using pH, temperature, mixing time, and the volume of Hexane. Likewise, it was also discovered by observation that oil and water could not combine. That is why, in order to breach the barrier, an organic solvent such as hexane was added to the heterogeneous mixture.

Electrical conductivity is a measurement of a solution's capacity to conduct electricity or pass electric flow, and

is determined by the dissociation of conductive ions from soluble salts and inorganic compounds such as alkalis, chlorides, sulphides, carbonate molecules, and temperature data (Zafar, Javed and Aly Hassan, 2022). The ionic conductivity of hydrocarbons is also important

in a variety of other applications, including petroleum processing and transformer oil uses. In the case of petroleum processing, for example, increased electrical conductivity is required to prevent an undesired build-up of electrostatic potential.

Table 5. Wastewater factors used before removal

Standard Order	Before Removal Parameters				
	pH	Temperature (°C)	Mixing Time (Minutes)	Organic Solvent Volume (mL)	Conductivity (mV)
1	12.00	50.00	30.00	4	-275
2	12.00	50.00	5.00	4	-236
3	12.00	5.00	30.00	20	-276
4	3.00	50.00	5.00	20	+267
5	12.00	5.00	5.00	20	-269
6	3.00	5.00	30.00	4	+147
7	3.00	50.00	30.00	20	+250
8	3.00	5.00	5.00	4	+200
9	3.00	27.50	17.50	12	+206
10	12.00	27.50	17.50	12	-342
11	7.50	5.00	17.50	12	-68
12	7.50	50.00	17.50	12	+45
13	7.50	27.50	5.00	12	-44
14	7.50	27.50	30.00	12	-2
15	7.50	27.50	17.50	4	-49
16	7.50	27.50	17.50	20	-49
17	7.50	27.50	17.50	12	-10
18	7.50	27.50	17.50	12	-46
19	7.50	27.50	17.50	12	-59
20	7.50	27.50	17.50	12	-60
21	7.50	27.50	17.50	12	-21

This is usually accomplished by the presence of particular substances. Sankaran *et al.* (2019) reported that Oils' electrical conductivity has often been linked to impurities or micro-constituents contained in them. One of the biggest contaminants in oil is dissolved water, which is suspected of having a substantial influence on the electrical conductivity of hydrocarbon liquids. From Table 5, it was noticed the dependence of conductivity on pH. While the pH was 3, conductivity became positively higher (+267 mV) compared to pH 12 where it was negatively lower (below -330 mV) before removal. And at pH 7.5, conductivity was between +50 and -70 mV. These variations were due to presence of conductive ions mentioned by Zafar,

Javed and Aly Hassan (2022). The effects of n-hexane on viscosity have been also investigated at 50 C. It can be observed that, at the same experimental temperature, a higher solvent content is better for reducing heavy oil viscosity. The reason for this is that the heavy oil has a high concentration of resin and asphaltene, and adding solvent to heavy oil can enhance the proportion of light components while decreasing viscosity. According to research, n-hexane can significantly improve the exploitation effect of heavy oil. The solubility of n-hexane in heavy oil decreases as temperature rises. The reason for this is that n-hexane's reduction effect can continue improving the flow capability of oil products in porous materials (Li and Sun, 2017).

Standard Order	After Removal Parameters Changes			Table 6. Measurements recorded after removal
	pH	Conductivity (mV)	Retention Time (Minutes)	
1	10.40	-190	10	
2	10.28	-169	12	
3	11.92	-274	25	
4	3.18	+214	12	
5	11.88	-250	2	
6	3.43	+142	25	
7	3.09	+238	7	
8	4.63	+146	2	
9	3.79	+184	4	
10	11.81	-273	15	
11	7.52	-22	2	
12	6.28	+53	8	
13	7.25	-7	2	
14	7.35	-14	2	
15	6.72	+28	2	
16	7.30	-9	2	
17	7.00	+8	3	
18	6.20	+60	2	
19	7.29	-6	2	
20	6.78	+23	3	
21	7.07	+2	2	

The acidity/basicity of the reaction medium is widely recognized to have a strong impact on the crystallization and development of inorganic-organic hybrid materials. On the basis of the acid-base concept, the amount of deprotonation of an organic ligand and, in certain cases, the production of an OH-ligand in aqueous system with regard to the pH of the reaction medium will favour the connection of polycarboxylate binder to metal atom. In conjunction to compositional criteria such as pH, solvents, and such as temperature, and time should also be considered while constructing synthetic methods. (Seetharaj *et al.*, 2019).

Heavy Metals Removal

The removal % of heavy metal ions (Cu^{2+} , Fe^{2+} , Pb^{2+}), retention duration, and pH and conductivity values after removal using chitosan membrane were reported in Table 7. After removal, the pH of the treated water solutions (Table 7) ranged from 3.09 to 11.92, the retention duration ranged from 2 to 11 minutes, and the conductivity ranged from -274 to +238 mV depending on whether the solution was acidic or basic. Cu^{2+} removal percentage was 98.71 (pH = 7.52 and conductivity = -22 mV), Fe^{2+} removal percentage was 98.29 (pH = 7.52 and conductivity = -22 mV), and

Pb^{2+} removal percentage was 98.77 (pH = 6.28 and conductivity = -53 mV).

And the results showed that the conductivity polarity was affected by the pH of the solution. The conductivity values were positive for acidic solutions and negative for basic solutions. According to Guo *et al.* (2022), the wastewater pH influences the adsorption effectiveness of the membrane. Once the pH of the fluid is less than 7.50, the fluid becomes positively charged. Whenever the pH of the fluid is more than 7.50, it becomes negatively charged. If the pH of the medium is lesser, the amount of H^+ in the mixture is high, and H^+ needs to compete for adsorption sites with metal ions Pb^{2+} . Simultaneously, the amino and carboxyl functional groups in the membranes are protonated, leading the material surface to become positively charged (Guo *et al.*, 2022). When the positively charged surface comes in direct contact with Pb^{2+} , they exhibit severe repulsive forces. Conversely, as the solution pH rises, the H^+ concentration decreased dramatically (Akbari Zadeh, Daghbandan and Abbasi Souraki, 2022; Guo *et al.*, 2022). The amino and carboxyl groups are dehydrogenated, leading to an increase in net negative charge. Extra metallic ions would become attached to the surface of the membrane due to electrostatic

attraction. Same situation would also be applied for Fe²⁺ (Akbari Zadeh, Daghbandan and Abbasi Souraki, 2022; Guo *et al.*, 2022). The higher the concentration of carboxyl and amino groups in a mixture, the more metallic ions are chelated well with carboxyl or amino

groups, and even the percentage removal steadily rises. At increased pH, a substantial number of metallic ions precipitate, affecting heavy metal ions sorption by the membrane (Guo *et al.*, 2022).

Standard Order	After Removal Parameters			Element Ions			Table 7. Heavy metals of Cu ²⁺ removal	of Fe
	pH	Conductivity (mV)	Retention Time (Minutes)	% R	% R	% R		
1	10.40	-190	10				75.25	71.4
2	10.28	-169	12				83.77	87.5
3	11.92	-274	25				73.29	80.4
4	3.18	+214	12				59.93	62.1
5	11.88	-250	2				78.55	79.2
6	3.43	+142	25				67.29	66.9
7	3.09	+238	7				61.23	63.9
8	4.63	+146	2				62.69	59.4
9	3.79	+184	4				66.78	70.6
10	11.81	-273	15				72.33	87.4
11	7.52	-22	2				94.71	90.9
12	6.28	+53	8				94.29	91.2
13	7.25	-7	2				98.21	96.1
14	7.35	-14	2				96.88	95.5
15	6.72	+28	2				97.71	92.8
16	7.30	-9	2				89.56	90.2
17	7.00	+8	3				94.55	96.2
18	6.20	+60	2				94.17	96.0
19	7.29	-6	2				94.27	96.0
20	6.78	+23	3				94.56	96.0
21	7.07	+2	2				94.45	96.5

According to Khatri, Tyagi and Rawtani (2017), Sidek, Ninie and Mohamad (2017), the phase volume fraction is a crucial consideration in the extraction process. To test the influence of the solvent hexane on oil removal efficiency, it could be said that the percent removal decreased dramatically as the phase volume ratios increased. The lower removal effectiveness might be attributed to the substantially larger amount of oil phase employed in this extraction. When Hexane volume was low in Table 7, the performance of the membrane removing oil was very good for Cu²⁺, Fe²⁺, Pb²⁺ (Khatri, Tyagi and Rawtani, 2017; Sidek, Ninie and Mohamad, 2017). Water in a mixed solvent solution can affect the solvation process and govern the development of various habitats. As the water/hexane ratio increases, the hexane particles are gradually replaced by water, demonstrating the clear link between the solvent ratio and the product composition (Seetharaj *et al.*, 2019).

Effects of Parameters using Chitosan Membrane

A. Response: %R of Cu – Analysis of variance (ANOVA) for Quadratic Model

The ANOVA evaluation of the CCD approach was shown in Table 8. The identified 1491.32 model F-value indicates that the model is significant. If the Prob > F value is less than 0.05, the control variables are all significant, indicating significant variables at the 95% confidence level (Prajapati *et al.*, 2022). A, C, D, A², C², D², AB, AC, BC and BD were significant terms in this case, while all other terms were insignificant. The model F-value was higher, indicating that this model was significant even if not all model terms were significant. Table 8 also displays the various values that have been used to evaluate the CCD method. The Value of R² was 0.9997, indicating that the model performed well in terms of fit and significance. The difference between

R^2 (0.9997) values and R^2_{Adj} (0.9990) values should be really small, indicating that the model is very powerful (Prajapati et al., 2022).

Table 8. ANOVA– %R of Cu^{2+}

Source	Sum of Squares	DF	Mean Square	F Value	Prob > F
Model	3813.86	14	272.42	1491.32	< 0.0001
A	15.40	1	15.40	84.31	< 0.0001
B	0.088	1	0.088	0.48	0.5131
C	8.48	1	8.48	46.44	0.0005
D	33.21	1	33.21	181.81	< 0.0001
A ²	1639.90	1	1639.90	8977.43	< 0.0001
B ²	0.41	1	0.41	2.24	0.1852
C ²	17.86	1	17.86	97.75	< 0.0001
D ²	4.09	1	4.09	22.37	0.0032
AB	6.89	1	6.89	37.71	0.0009
AC	48.41	1	48.41	265.03	< 0.0001
AD	4.000×10 ⁻⁵	1	4.000×10 ⁻⁵	2.190×10 ⁻⁴	0.9887
BC	5.38	1	5.38	29.45	0.0016
BD	35.19	1	35.19	192.66	< 0.0001
CD	2.000×10 ⁻⁴	1	2.000×10 ⁻⁴	1.095×10 ⁻³	0.9747
Residual	1.10	6	0.18		
Lack of Fit	0.98	2	0.49	16.21	0.0121
Pure Error	0.12	4	0.030		
Cor Total	3814.96	20			

Std. Dev.	0.43	R^2	0.9997
Mean	83.07	R^2_{Adj}	0.9990
C.V.	0.51	R^2_{Pred}	0.9612
PRESS	147.98	Adeq Precision	106.074

Factor	Coefficient Estimate	DF	Standard Error	95% CI Low	95% CI High	VIF
Intercept	94.67	1	0.14	94.33	95.02	
A – pH	2.78	1	0.30	2.04	3.51	5.00
B – Temperature	-0.21	1	0.30	-0.95	0.53	5.00
C – Time	-0.92	1	0.14	-1.25	-0.59	1.00
D – Solvent	-4.08	1	0.30	-4.81	-3.34	5.00
A ²	-25.35	1	0.27	-26.00	-24.69	2.05
B ²	-0.40	1	0.27	-1.05	0.25	2.05
C ²	2.64	1	0.27	1.99	3.30	2.05
D ²	-1.27	1	0.27	-1.92	-0.61	2.05
AB	-2.08	1	0.34	-2.90	-1.25	5.00
AC	-2.46	1	0.15	-2.83	-2.09	1.00
AD	-5.000×10 ⁻³	1	0.34	-0.83	0.82	5.00
BC	-0.82	1	0.15	-1.19	-0.45	1.00
BD	-4.69	1	0.34	-5.52	-3.86	5.00
CD	-5.000×10 ⁻³	1	0.15	-0.37	0.36	1.00

DOI: [10.6092/issn.2281-4485/16047](https://doi.org/10.6092/issn.2281-4485/16047)**Final equation in terms of coded factors:**

$$\begin{aligned} \%R \text{ of Cu} = & 94.67 + 2.78A - 0.21B - 0.92C - \\ & 4.08D - 25.35A^2 - 0.40B^2 + 2.64C^2 - 1.27D^2 - \\ & 2.08AB - 2.46AC - 5.000 \times 10^{-3} AD - 0.82BC \\ & - 4.69BD - 5.000 \times 10^{-3} CD \end{aligned} \quad [2]$$

Final equation in terms of actual factors:

$$\begin{aligned} \%R \text{ of Cu} = & 9.05062 + 20.72151 \text{ pH} + 0.55154 \\ & \text{Temperature} - 0.25733 \text{ Time} + 0.68354 \text{ Solvent} \\ & - 1.25162 \text{ pH}^2 - 7.90627 \times 10^{-4} \text{ Temperature}^2 \\ & + 0.016926 \text{ Time}^2 - 0.019770 \text{ Solvent}^2 - \\ & 0.020494 \text{ pH} \times \text{Temperature} - 0.043733 \\ & \text{pH} \times \text{Time} - 1.38889 \times 10^{-4} \text{ pH} \times \text{Solvent} - \\ & 2.91556 \times 10^{-3} \text{ Temperature} \times \text{Time} - 0.026056 \\ & \text{Temperature} \times \text{Solvent} - 5.00000 \times 10^{-5} \\ & \text{Time} \times \text{Solvent} \end{aligned} \quad [3]$$

Adequate precision (106.074) is used to evaluate signal to noise ratio, but this proportion should always be greater than 4, which is the case here (Table 8), indicating that the design are significant (Prajapati *et al.*, 2022). As seen Figure 4.28, the predicted values are linearly distributed near the experimental yield, indicating that all three methods' predicted models are good.

As seen in Figure 6, perturbation of effects variables for %R of Cu using 8 g Chitosan membrane. pH (factor B) had the greatest influence on the inverse of this response (%R of Cu). The 3D response surface plots of the Response against two variables (%R of Cu) could be seen in Figure 7. The pH value had a significant impact the removal of Cu^{2+} .

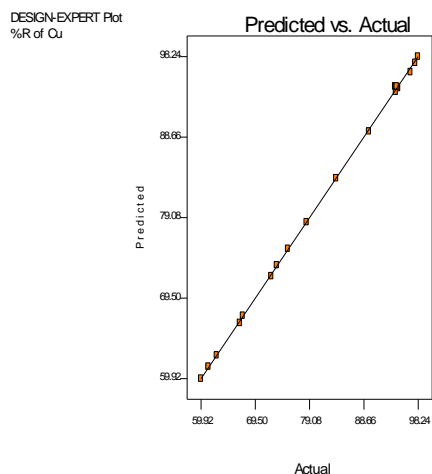


Figure 5. Plot of predicted vs actual (%R Cu^{2+})

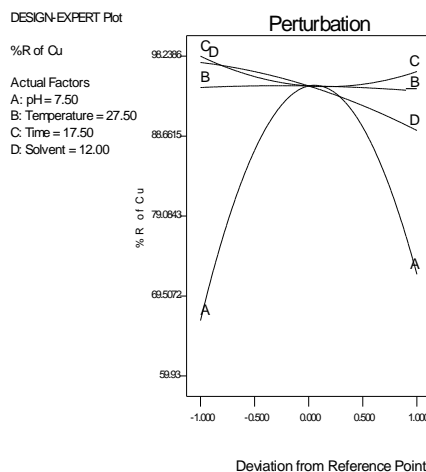


Figure 6. Perturbation plot of effects of variables (%R of Cu)

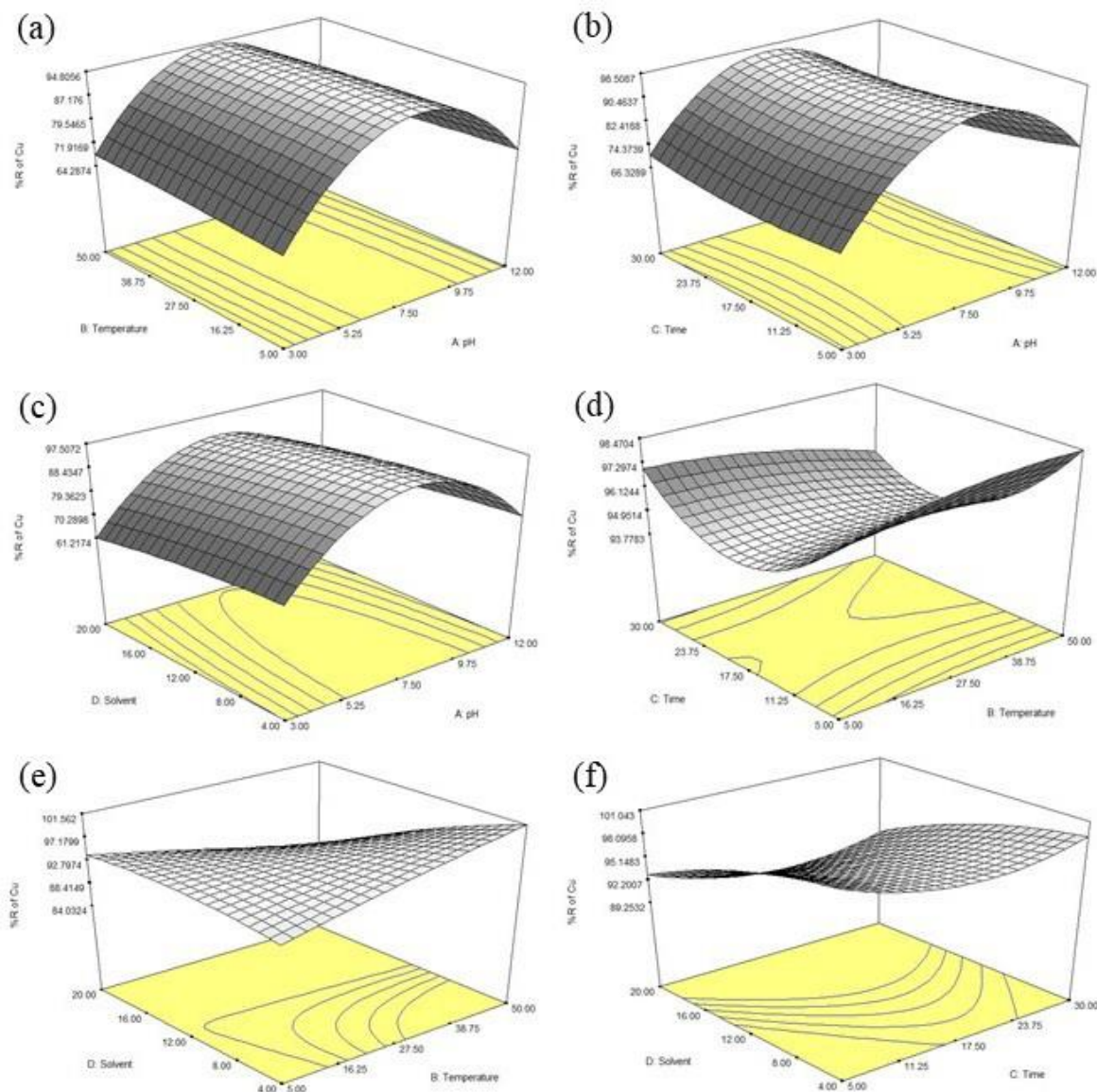


Figure 7. (a-f) 3D Response vs two variables (%R of Cu).

B. Response: %R of Fe – Analysis of variance (ANOVA) for Quadratic Model

The F-test for ANOVA was used to determine the statistical significance of the model equation, which revealed that the regression is statistically significant at 95 % ($p < 0.05$) confidence level. ANOVA for nitrate reductase production revealed that the model's "F-value" was 755.09, and the "Prob > F-value" value was 0.0001, indicating that the model was very significant (Table 4.20). The statistically significant terms were A, C, D, A^2 , B^2 , D^2 , AB, AC, BC and CD

since their Prob > F – value was less than 0.05. The coefficient of determination (R^2) was determined as 0.9994, demonstrating high agreement between actual and projected values. "Adeq. Precision" calculated the signal-to-noise (deviation) ratio. A ratio larger than 4 is preferred. Because the ratio of 78.088 suggests an appropriate signal, the model is statistically significant for the function (Vaidyanathan *et al.*, 2010). The R^2_{Adj} (0.9981) corrected the R^2 value (0.9994). Following the formulation of RSM model regression, Equations (4) and (5) were generated.

Table 9. ANOVA– %R of Fe²⁺

Source	Sum of Squares	DF	Mean Square	F Value	Prob > F
Model	3411.29	14	243.66	755.09	< 0.0001
A	141.12	1	141.12	437.31	< 0.0001
B	0.045	1	0.045	0.14	0.7217
C	4.12	1	4.12	12.77	0.0117
D	3.35	1	3.35	10.39	0.0180
A ²	691.86	1	691.86	2143.99	< 0.0001
B ²	49.93	1	49.93	154.73	< 0.0001
C ²	0.32	1	0.32	0.98	0.3598
D ²	40.39	1	40.39	125.16	< 0.0001
AB	2.85	1	2.85	8.82	0.0250
AC	73.75	1	73.75	228.54	< 0.0001
AD	0.14	1	0.14	0.43	0.5373
BC	65.72	1	65.72	203.67	< 0.0001
BD	0.025	1	0.025	0.076	0.7921
CD	16.73	1	16.73	51.85	0.0004
Residual	1.93	6	0.32		
Lack of Fit	1.73	2	0.87	16.90	0.0112
Pure Error	0.20	4	0.051		
Cor Total	3413.23	20			

Std. Dev.	0.57	R ²	0.9994
Mean	84.15	R ² _{Adj}	0.9981
C.V.	0.68	R ² _{Pred}	0.9243
PRESS	258.29	Adeq Precision	78.088

Factor	Coefficient Estimate	DF	Standard Error	95% CI Low	95% CI High	VIF
Intercept	95.82	1	0.19	95.36	96.28	
A – pH	8.40	1	0.40	7.42	9.38	5.00
B – Temperature	0.15	1	0.40	-0.83	1.13	5.00
C – Time	-0.64	1	0.18	-1.08	-0.20	1.00
D – Solvent	-1.30	1	0.40	-2.28	-0.31	5.00
A ²	-16.46	1	0.36	-17.33	-15.59	2.05
B ²	-4.42	1	0.36	-5.29	-3.55	2.05
C ²	0.35	1	0.36	-0.52	1.22	2.05
D ²	-3.98	1	0.36	-4.85	-3.11	2.05
AB	-1.33	1	0.45	-2.43	-0.23	5.00
AC	-3.04	1	0.20	-3.53	-2.54	1.00
AD	0.29	1	0.45	-0.81	1.39	5.00
BC	-2.87	1	0.20	-3.36	-2.37	1.00
BD	0.12	1	0.45	-0.98	1.22	5.00
CD	1.45	1	0.20	0.95	1.94	1.00

Final Equation in Terms of Coded Factors:

$$\begin{aligned} \%R \text{ of Fe} = & 95.82 + 8.40A + 0.15B - 0.64C \\ & - 1.30D - 16.46A^2 - 4.42B^2 + 0.35C^2 - 3.98D^2 \\ & - 1.33 AB - 3.04 AC + 0.29 AD - 2.87 BC + \\ & 0.12 BD + 1.45 CD \end{aligned} \quad [4]$$

Final Equation in Terms of Actual Factors:

$$\begin{aligned} \%R \text{ of Fe} = & 13.17571 + 15.27007 \text{ pH} \\ & + 0.75603 \text{ Temperature} + 0.38122 \\ & \text{Time} + 0.99650 \text{ Solvent} - 0.81296 \text{ pH}^2 - \\ & 8.73583 \times 10^{-3} \text{ Temperature}^2 + 2.25590 \times 10^{-3} \\ & \text{Time}^2 - 0.062149 \text{ Solvent}^2 - 0.013173 \\ & \text{pH} \times \text{Temperature} - 0.053978 \text{ pH} \times \text{Time} \\ & + 8.15972 \times 10^{-3} \text{ pH} \times \text{Solvent} - 0.010191 \\ & \text{Temperature} \times \text{Time} + 6.87500 \times 10^{-4} \\ & \text{Temperature} \times \text{Solvent} + 0.014463 \\ & \text{Time} \times \text{Solvent} \end{aligned} \quad [5]$$

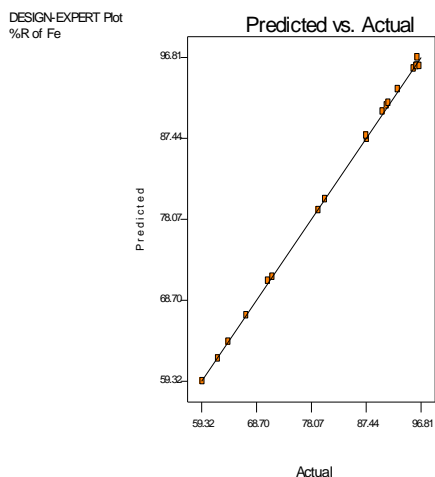


Figure 8. Plot of predicted vs actual (%R of Fe)

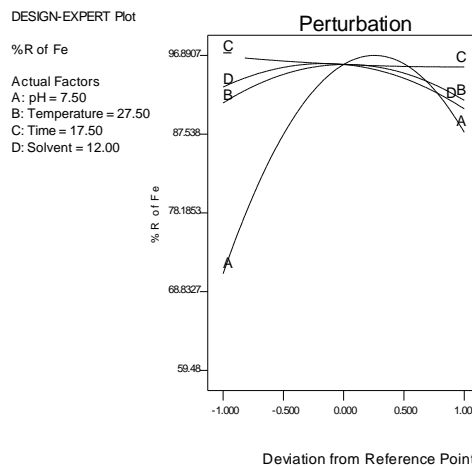


Figure 9. Perturbation plot of effects of variables (%R of Fe)

Figure 8 was the plot of predicted against actual values for the %R of Fe using 8 g Chitosan membrane. All the points in the graph had contact with the line which showed the significance of the model.

According to the perturbation plot (Figure 9), pH (A) had a substantial influence on the %R of Fe when compared to other factors. The perturbation graph clearly demonstrates that the three components

temperature (B), time (C), and solvent (D) had no significant impact in the removal. A perturbation plot is a useful diagrammatic form for comparing the impacts of all parameters at a certain location in the design space. The response is plotted by varying only one element while maintaining the others constant (Nwobi-Okoye and Uzochukwu, 2020) artificial neural network (ANN).

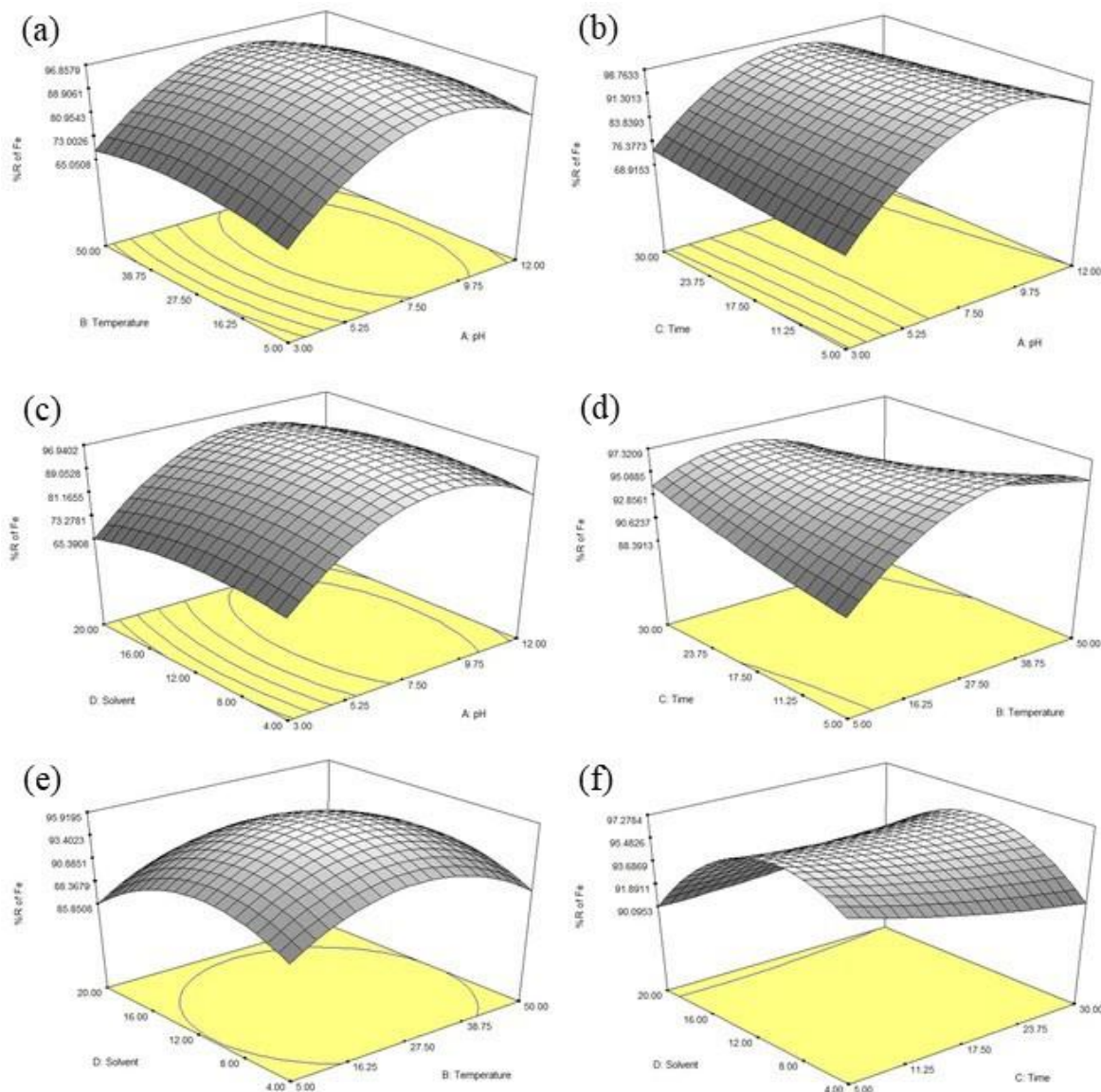


Figure 10. (a-f) 3D Response vs two variables (%R of Fe)

Figure 10 has showed the 3D Response against two variables for %R of Fe using Chitosan membrane. The influence of pH, temperature, time and solvent factors interacting on the %R of Fe (z-axis) was examined by showing three-dimensional response surface graphs against any independent factors while maintaining the other independent variable at its central level.

C. Response: %R of Pb – Analysis of variance (ANOVA) for Quadratic Model

Table 10 displays the ANOVA for %R of Pb that was used to obtain Equations (6) and (7). The Model F-value of 941.56, as given in Table 10 indicated that the model was significant. “Prob > F” values less than 0.0500 indicated that model terms were significant. As a result, in this situation, A, C, AB, AC, BC, BD, CD A², B², C² and D² were important model terms.

Table 10. ANOVA – %R of Pb²⁺

Source	Sum of Squares	DF	Mean Square	F Value	Prob >F
Model	3030.01	14	216.43	941.56	< 0.0001
A	395.65	1	395.65	1721.24	< 0.0001
B	0.72	1	0.72	3.13	0.1272
C	20.31	1	20.31	88.34	< 0.0001
D	0.26	1	0.26	1.13	0.3291
A ²	993.85	1	993.85	4423.66	< 0.0001
B ²	54.82	1	54.82	238.49	< 0.0001
C ²	9.06	1	9.06	39.42	0.0008
D ²	18.97	1	18.97	82.53	< 0.0001
AB	17.70	1	17.70	77.01	0.0001
AC	20.58	1	20.58	89.51	< 0.0001
AD	0.11	1	0.11	0.47	0.5203
BC	57.19	1	57.19	248.81	< 0.0001
BD	29.53	1	29.53	128.48	< 0.0001
CD	34.40	1	34.40	149.67	< 0.0001
Residual	1.38	6	0.23		
Lack of Fit	1.05	2	0.53	6.46	0.0558
Pure Error	0.33	4	0.081		
Cor Total	3031.39	20			

Std. Dev.	0.48	R ²	0.9995
Mean	86.05	R ² _{Adj}	0.9985
C.V.	0.56	R ² _{Pred}	0.9463
PRESS	162.84	Adeq Precision	96.323

Factor	Coefficient Estimate	DF	Standard Error	95% CI Low	95% CI High	VIF
Intercept	93.64	1	0.16	93.26	94.03	
A – pH	14.07	1	0.34	13.24	14.89	5.00
B – Temperature	0.60	1	0.34	-0.23	1.43	5.00
C – Time	1.42	1	0.15	1.05	1.80	1.00
D – Solvent	-0.36	1	0.34	-1.19	0.47	5.00
A ²	-19.73	1	0.30	-20.47	-19.00	2.05
B ²	4.63	1	0.30	3.90	5.37	2.05
C ²	1.88	1	0.30	1.15	2.62	2.05
D ²	-2.73	1	0.30	-3.46	-1.99	2.05
AB	-3.33	1	0.38	-4.25	-2.40	5.00
AC	-1.60	1	0.17	-2.02	-1.19	1.00
AD	0.26	1	0.38	-0.67	1.19	5.00
BC	2.67	1	0.17	2.26	3.09	1.00
BD	4.30	1	0.38	3.37	5.22	5.00
CD	2.07	1	0.17	1.66	2.49	1.00

The “Lack of Fit F-value” of 1.05 in Table 10 indicated that the Lack of Fit was not significant in comparison to the pure error (0.33) and R² (0.9995), R²_{Adj} (0.9985) and R²_{Pred} (0.9463) had close values.

Final Equation in Terms of Coded Factors:

$$\begin{aligned} \%R \text{ of Pb} = & 93.64 + 14.07 A + 0.60 B + 1.42 \\ & C - 0.36 D - 19.73 A^2 + 4.63 B^2 + 1.88C^2 - 2.73 \\ & D^2 - 3.33 AB - 1.60 AC + 0.26 AD + 2.67 BC \\ & + 4.30 BD + 2.07 CD \end{aligned} \quad [6]$$

Final Equation in Terms of Actual Factors:

$$\begin{aligned} \%R \text{ of Pb} = & 24.62234 + 19.05720 \\ & \text{pH} - 0.68318 \text{ Temperature} - 0.60448 \\ & \text{Time} - 0.095951 \text{ Solvent} - 0.97437 \\ & \text{pH}^2 + 9.15367 \times 10^{-3} \text{ Temperature}^2 + \\ & 0.012058 \text{ Time}^2 - 0.042593 \text{ Solvent}^2 - \\ & 0.032852 \text{ pH} \times \text{Temperature} - 0.028511 \\ & \text{pH} \times \text{Time} + 7.18750 \times 10^{-3} \text{ pH} \times \text{Solvent} \\ & + 9.50667 \times 10^{-3} \text{ Temperature} \times \text{Time} + \\ & 0.023868 \text{ Temperature} \times \text{Solvent} + 0.020738 \\ & \text{Time} \times \text{Solvent} \end{aligned} \quad [7]$$

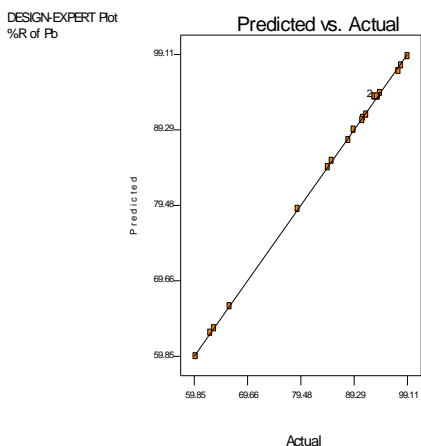


Figure 11. Plot of predicted vs actual (%R of Pb)

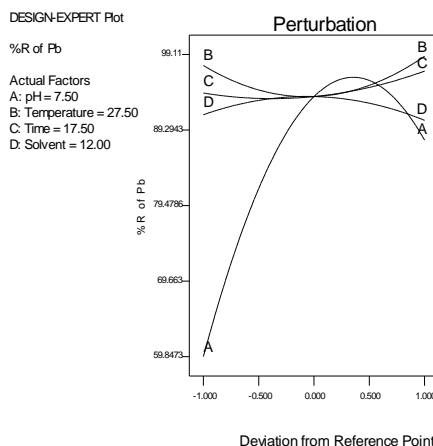


Figure 12. Perturbation plot of effects of variables (%R of Pb)

The plotting of experimental responses against expected responses in Figure 11 demonstrated that there was a very excellent correlation between the actual and the model - predicted values, and the model exhibits no modification of the standard deviation.

Figure 12 showed the perturbation plot of effects of variables for the %R of Pb using Chitosan membrane. Like in previous perturbation graphs in this study, the sheerness of curve of a particular component indicates the responsiveness to changes through one variable. Thus, relatively flat lines indicate a general lack of meaningful influence upon that response by fluctuation in the component under consideration (Mishra *et al.*, 2018)effect of various factors like light

intensity, agitation rate and dilution of DPOME on the hydrogen productivity of *Rhodospseudomonas palustris* were investigated using batch system. Investigation methods like response surface methodology (RSM. This perturbation plot was employed in the current study to assess %R of Pb as four variables (pH, temperature, time and solvent) were tested using Central Composite Design of the Response Surface Methodology. In Figure 13, at pH 12 or above, the precipitation of metal salt to $M(OH)_2$, which was unable to engage in the process, resulted in a low dimensional structure. These metal salts not only generate a basic environment that promotes deprotonation, but they also participate in coordination (Seetharaj *et al.*, 2019).

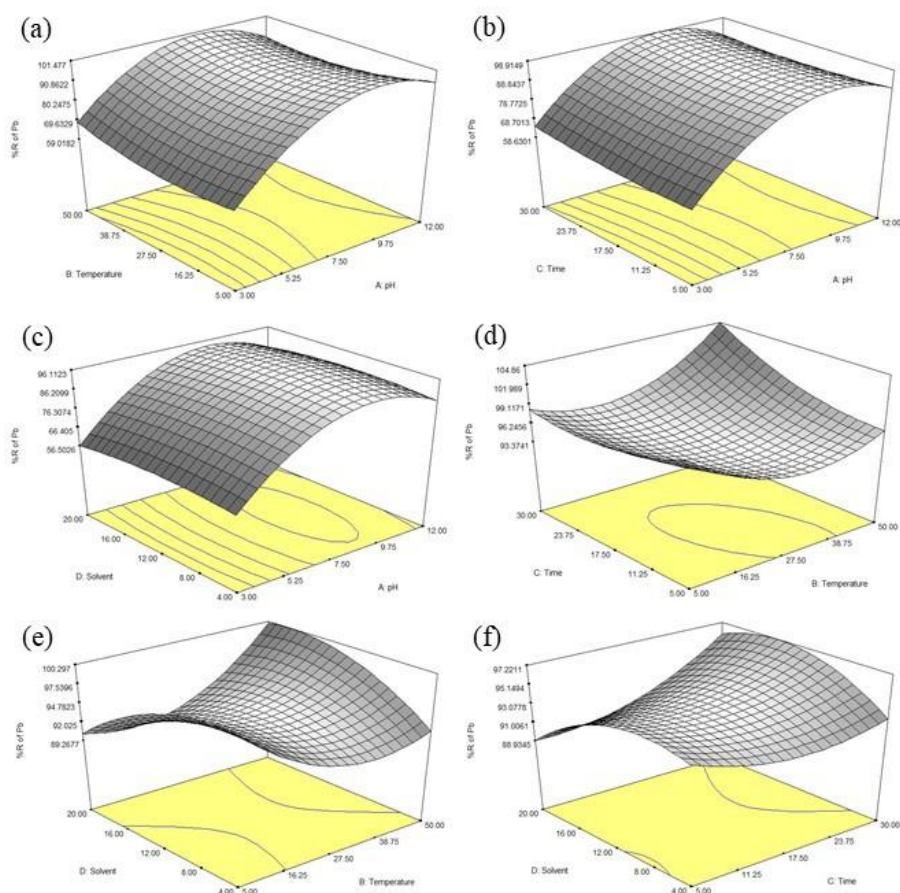


Figure 13. (a-f) 3D Response vs two variables (%R of Pb)

Conclusion

This work studied the effect of pH, temperature, time and hexane as factors on the ecologically friendly removal of heavy metals from oily wastewater using modified chitosan. Chitosan has been effectively modified using cellulose and gelatin. Chitosan was characterized using Fourier Transform Infrared (FTIR), Scanning Electron Microscopy (SEM), and X-Ray Diffraction (XRD). We investigated the effects of pH solution and conductivity. Adsorption was carried out in order to remove the heavy metals. The clearance percentages were greater than 90%, especially when the starting pH was 7.50 and the amount of Hexane was 12 mL. The % of Cu^{2+} removed was 98.71 (pH = 7.52 and conductivity = -22

mV), the % of Fe^{2+} removed was 98.29 (pH = 7.52 and conductivity = -22 mV), and the % of Pb^{2+} removed was 98.77 (pH = 6.28 and conductivity = -53 mV). As the temperature rises, the solubility of n-hexane in heavy oil drops. The reason for this is that the reducing impact of n-hexane can continue to improve the flow capacity of oil products in porous surfaces.

Acknowledgments

The author would like to thank the Vaal University of Technology's Department of Chemical & Metallurgical Engineering for providing continuous operating facilities, as well as his supervisor and co-supervisor for continual remarks and corrections.

DOI: [10.6092/issn.2281-4485/16047](https://doi.org/10.6092/issn.2281-4485/16047)

References

- ABDEL-HAKIM A., ABDELLA A.H., SABAA M.W., GOHAR H.Y., MOHAMED R.R., TERA FM. (2021) Performance evaluation of modified fabricated cotton membrane for oil/water separation and heavy metal ions removal. *Journal of Vinyl and Additive Technology*, 27(4):933–945. Doi: [10.1002/vnl.21866](https://doi.org/10.1002/vnl.21866)
- ADELEYE A.O., NKEREUEM M.E., OMOKHUDU G.I., AMOO A.O., SHIAKA G.P., YERIMA M.B. (2018) Effect of microorganisms in the bioremediation of spent engine oil and petroleum related environmental pollution. *Journal of Applied Sciences and Environmental Management*, 22(2):157. Doi: [10.4314/jasem.v22i2.1](https://doi.org/10.4314/jasem.v22i2.1)
- AKBARI ZADEH M., DAGHBANDAN A., ABBASI SOURAKI B. (2022) Removal of iron and manganese from groundwater sources using nano-biosorbents. *Chemical and Biological Technologies in Agriculture*, 9(1):1–14. Doi: [10.1186/s40538-021-00268-x](https://doi.org/10.1186/s40538-021-00268-x)
- CHEN Q., YE Z., TANG L., WU T., JIANG Q., LAI N. (2020) Synthesis and solution properties of a novel hyperbranched polymer based on chitosan for enhanced oil recovery. *Polymers*, 12(9):1–24. Doi: [10.3390/POLYM12092130](https://doi.org/10.3390/POLYM12092130)
- CHIONO V., PULIERI E., VOZZI G., CIARDELLI G., AHLUWALIA A., GIUSTI P. (2008) Genipin-crosslinked chitosan/gelatin blends for biomedical applications', *Journal of Materials Science: Materials in Medicine*, 19(2):889–898. Doi: [10.1007/s10856-007-3212-5](https://doi.org/10.1007/s10856-007-3212-5)
- DESHMUKH K., AHAMED M.B., DESHMUKH R.R., PASHA S.K.K., BHAGAT P.R., CHIDAMBARAM K. (2017) 'Biopolymer Composites With High Dielectric Performance: Interface Engineering', *Biopolymer Composites in Electronics*, pp. 27–128. Doi: [10.1016/B978-0-12-809261-3.00003-6](https://doi.org/10.1016/B978-0-12-809261-3.00003-6)
- DOSHIA B., REPOA E., HEISKANEN J.P., ANTTI J., SILLANPÄÄ S.M. (2017) 'Effectiveness of N,O-carboxymethyl chitosan on destabilization of Marine Diesel, Diesel and Marine-2T oil for oil spill treatment. *Carbohydrate Polymers*, 167:326–336. Doi: [10.1016/j.carbpol.2017.03.064](https://doi.org/10.1016/j.carbpol.2017.03.064)
- FATHY M., SELIM H., SHAHAWY A.E.L. (2020) Chitosan/MCM-48 nanocomposite as a potential adsorbent for removing phenol from aqueous solution. *RSC Advances*, 10(39):23417–23430. Doi: [10.1039/d0ra02960b](https://doi.org/10.1039/d0ra02960b)
- FIDELES T.B., SANTOS J.L., TOMÁS H., FURTADO G.T.F.S., LIMA D.B., BORGES S.M.P., FOOK M.V.L. (2018) Characterization of Chitosan Membranes Crosslinked by Sulfuric Acid. *OALib*, 05(01):1–13. Doi: [10.4236/oalib.1104336](https://doi.org/10.4236/oalib.1104336)
- GUO W., GUO R., PEI H., WANG B., LIU N., MO Z. (2022) 'Electrospinning PAN/PEI/MWCNT-COOH nanocomposite fiber membrane with excellent oil-in-water separation and heavy metal ion adsorption capacity', *Colloids and Surfaces A: Physicochemical and Engineering Aspects*, 641:128557. Doi: [10.1016/j.colsurfa.2022.128557](https://doi.org/10.1016/j.colsurfa.2022.128557)
- ISLAM B. (2015) Petroleum sludge, its treatment and disposal: A review. *International Journal of Chemical Sciences*, 13(4):1584–1602.
- ISLAM S., ARNOLD L., PADHYE R. (2015) Comparison and characterisation of regenerated chitosan from 1-butyl-3-methylimidazolium chloride and chitosan from crab shells. *BioMed Research International*, 1–6. Doi: [10.1155/2015/874316](https://doi.org/10.1155/2015/874316)
- KHALIFAA R.E., OMERA A.M., TAMERA T.M., ALIB A.A., AMMARC Y.A., MOHY M.S.E. (2019) Efficient eco-friendly crude oil adsorptive chitosan derivatives: Kinetics, equilibrium and thermodynamic studies. *Desalination and Water Treatment*, 159:269–281. Doi: [10.5004/dwt.2019.24166](https://doi.org/10.5004/dwt.2019.24166)
- KHATRI N., TYAGI S., RAWTANI D. (2017) Recent strategies for the removal of iron from water: A review', *Journal of Water Process Engineering*, 19(13):291–304. Doi: [10.1016/j.jwpe.2017.08.015](https://doi.org/10.1016/j.jwpe.2017.08.015)
- LAKRA R., BALAKRISHNAN M., BASU S. (2021) Development of cellulose acetate-chitosan-metal organic framework forward osmosis membrane for recovery of water and nutrients from wastewater. *Journal of Environmental Chemical Engineering*, 9(5):105882. Doi: [10.1016/j.jece.2021.105882](https://doi.org/10.1016/j.jece.2021.105882)

DOI: [10.6092/issn.2281-4485/16047](https://doi.org/10.6092/issn.2281-4485/16047)

- LIS., LI Z., SUN X. (2017) Effect of flue gas and n-hexane on heavy oil properties in steam flooding process. *Fuel*, 187:84–93. Doi: [10.1016/j.fuel.2016.09.050](https://doi.org/10.1016/j.fuel.2016.09.050)
- LIMA M.S.P., FREIRE M.S., FONSECA J.L.C., PEREIRA M.R. (2009) Chitosan membranes modified by contact with poly(acrylic acid). *Carbohydrate Research*, 344(13):1709–1715. Doi: [10.1016/j.carres.2009.05.024](https://doi.org/10.1016/j.carres.2009.05.024)
- MA Z., REN L.F., YING D., JIA J., SHAO J. (2022) ‘Sustainable electrospray polymerization fabrication of thin-film composite polyamide nanofiltration membranes for heavy metal removal’, *Desalination*, 539:115952. Doi: [10.1016/j.desal.2022.115952](https://doi.org/10.1016/j.desal.2022.115952)
- MARAFI A., ALBAZZAZ H., RANA M.S. (2019) Hydroprocessing of heavy residual oil: Opportunities and challenges’, *Catalysis Today*, 329:125–134. Doi: [10.1016/J.CATTOD.2018.10.067](https://doi.org/10.1016/J.CATTOD.2018.10.067)
- MISHRA P., SINGH L., WAHID Z.A, KRISHNAN S., RANA S., ISLAM M.A., SAKINAH M., AMEEN F., SYED A. (2018) Photohydrogen production from dark-fermented palm oil mill effluent (DPOME) and statistical optimization: Renewable substrate for hydrogen. *Journal of Cleaner Production*, 199:11–17. Doi: [10.1016/j.jclepro.2018.07.028](https://doi.org/10.1016/j.jclepro.2018.07.028)
- MITURA S., SIONKOWSKA, A., JAISWAL A. (2020) Biopolymers for hydrogels in cosmetics: review. *Journal of Materials Science: Materials in Medicine*, 31(6). Doi: [10.1007/s10856-020-06390-w](https://doi.org/10.1007/s10856-020-06390-w)
- MRUTHUNJAYAPPA M.H., SHARMA V.T., DHARMALINGAM K., KOTRAPPAVAR N.S., MONDAL D. (2020) Engineering a Biopolymer-Based Ultrafast Permeable Aerogel Membrane Decorated with Task-Specific Fe-Al Nanocomposites for Robust Water Purification. *ACS Applied Bio Materials*, 3(8): 5233–5243. Doi: [10.1021/acsabm.0c00630](https://doi.org/10.1021/acsabm.0c00630)
- NWOBI-OKOYE C.C., UZOCHUKWU C.U. (2020) RSM and ANN modeling for production of Al 6351/ egg shell reinforced composite: Multi objective optimization using genetic algorithm’, *Materials Today Communications*, 22:100674. Doi: [10.1016/j.mtcomm.2019.100674](https://doi.org/10.1016/j.mtcomm.2019.100674)
- OMER A.M., EWEIDA B.Y., TAMER T.M., SOLIMAN H.M.A., ALI S.M., ZAATOT A.A., MOHYELDIN M.S. (2021) ‘Removal of oil spills by novel developed amphiphilic chitosan-g-citronellal schiff base polymer’, *Scientific Reports*, 11(1), pp. 1–16. Doi: [10.1038/s41598-021-99241-9](https://doi.org/10.1038/s41598-021-99241-9)
- PRAJAPATI N., OZA S., KODGIRE P., KACHHWAHA S.S. (2022) ‘Microwave assisted biodiesel production: Assessment of optimization via RSM techniques’, *Materials Today: Proceedings*, 57, pp. 1637–1644. Doi: [10.1016/j.matpr.2021.12.243](https://doi.org/10.1016/j.matpr.2021.12.243)
- RAYHANI M., SIMJOO M., CHAHARDOWLI M. (2022) Effect of water chemistry on the stability of water-in-crude oil emulsion: Role of aqueous ions and underlying mechanisms. *Journal of Petroleum Science and Engineering*, 211: 110123. Doi: [10.1016/j.petrol.2022.110123](https://doi.org/10.1016/j.petrol.2022.110123)
- SAKWANICHOL J., SUNGTHONGJEEN S., PUTTIPIPATKHACHORN S. (2019) Preparation and characterization of chitosan aqueous dispersion as a pharmaceutical film forming material. *Journal of Drug Delivery Science and Technology*, 54:101230. Doi: [10.1016/J.JDDST.2019.101230](https://doi.org/10.1016/J.JDDST.2019.101230)
- SANKARAN A., STASZEL C., BELKNAP D., YARIN A.L., MASHAYEK F. (2019) Effect of atmospheric humidity on electrical conductivity of oil and implications in electrostatic atomization. *Fuel*, 253:283–292. Doi: [10.1016/j.fuel.2019.05.013](https://doi.org/10.1016/j.fuel.2019.05.013)
- SEETHARAJ R., VANDANA P.V., ARYA P., MATHEW S. (2019) Dependence of solvents, pH, molar ratio and temperature in tuning metal organic framework architecture. *Arabian Journal of Chemistry*, 12(3):295–315. Doi: [10.1016/j.arabjc.2016.01.003](https://doi.org/10.1016/j.arabjc.2016.01.003)
- SIDEK N., NINIE N.S., MOHAMAD S. (2017) Efficient removal of phenolic compounds from model oil using benzyl Imidazolium-based ionic liquids. *Journal of Molecular Liquids*, 240:794–802. Doi: [10.1016/j.molliq.2017.05.111](https://doi.org/10.1016/j.molliq.2017.05.111)
- DA SILVA I.C.G., LIMA B.N.B., CARNEIRO W.F., DE CARVALHO Y.G.Q., ELIAS C.R.M. (2013) ‘Chitosan microspheres applied for removal of oil from produced water in the oil industry’, *Polimeros*, 23(6), pp. 705–711. Doi: [10.4322/polimeros.2014.008](https://doi.org/10.4322/polimeros.2014.008)

DOI: [10.6092/issn.2281-4485/16047](https://doi.org/10.6092/issn.2281-4485/16047)

- TIWARIS., HASAN A., PANDEYL.M. (2017) A novel bio-sorbent comprising encapsulated *Agrobacterium fabrum* (SLAJ731) and iron oxide nanoparticles for removal of crude oil co-contaminant, lead Pb(II). *Journal of Environmental Chemical Engineering*, 5(1):442–452. Doi: [10.1016/j.jece.2016.12.017](https://doi.org/10.1016/j.jece.2016.12.017)
- VAIDYANATHAN R., GOPALRAM S., KALISHWARALAL K., DEEPAK V., PANDIAN S.R.K., GURUNATHAN S. (2010) ‘Enhanced silver nanoparticle synthesis by optimization of nitrate reductase activity’, *Colloids and Surfaces B: Biointerfaces*, 75(1), pp. 335–341. Doi: [10.1016/j.colsurfb.2009.09.006](https://doi.org/10.1016/j.colsurfb.2009.09.006)
- WANG D., ZHAO T., YAN L., MI Z., GU Q., ZHANG Y. (2016) ‘Synthesis, characterization and evaluation of dewatering properties of chitosan-grafting DMDAAC flocculants’, *International Journal of Biological Macromolecules*, 92, pp. 761–768. Doi: [10.1016/j.ijbiomac.2016.07.087](https://doi.org/10.1016/j.ijbiomac.2016.07.087)
- WOLOKE E., BARAFI J., JOSHI N., GIRIMONTE R., CHAKRABORTY, S. (2020) ‘Study of bio-materials for removal of the oil spill’, *Arabian Journal of Geosciences*, 13(23). Doi: [10.1007/s12517-020-06244-3](https://doi.org/10.1007/s12517-020-06244-3)
- GANG XIAO YAOQIANG WANG SHENGNAN XU PEIFENG LI CHEN YANG YU JIN QIUFENG SUN HAIJIA SU (2019) ‘Superior adsorption performance of graphitic carbon nitride nanosheets for both cationic and anionic heavy metals from wastewater’, *Chinese Journal of Chemical Engineering*, 27(2), pp. 305–313. Doi: [10.1016/J.CJCHE.2018.09.028](https://doi.org/10.1016/J.CJCHE.2018.09.028)
- YU P., WANG X., ZHANG K., WU M., WU Q., LIU J., YANG J., ZHANG J. (2020) ‘Continuous purification of simulated wastewater based on rice straw composites for oil/water separation and removal of heavy metal ions’, *Cellulose*, 27(9);5223–5239. Doi: [10.1007/s10570-020-03135-4](https://doi.org/10.1007/s10570-020-03135-4)
- ZAFAR A.M., JAVED M. A., HASSAN A.A. (2022) Unprecedented biodesalination rates–Shortcomings of electrical conductivity measurements in determining salt removal by algae and cyanobacteria’, *Journal of Environmental Management*, 302(PA):113947. Doi: [10.1016/j.jenvman.2021.113947](https://doi.org/10.1016/j.jenvman.2021.113947)
- ZAKUWAN S.Z., AHMAD I., TAHRIM N.A., MOHAMED F. (2021) Functional hydrophilic membrane for oil–water separation based on modified bio-based chitosan–gelatin’, *Polymers*, 13(7);1–20. Doi: [10.3390/polym13071176](https://doi.org/10.3390/polym13071176)
- ZHAO S., TAO Z., CHEN L., HAN M., ZHAO B., TIAN X., WANG L., MENG F. (2021) An antifouling catechol/chitosan-modified polyvinylidene fluoride membrane for sustainable oil-in-water emulsions separation’, *Frontiers of Environmental Science and Engineering*, 15(4). Doi: [10.1007/s11783-020-1355-5](https://doi.org/10.1007/s11783-020-1355-5)
- ZHU Z., JIANG L., LIU J., HE S., SHAO W. (2021) Sustainable, highly efficient and superhydrophobic fluorinated silica functionalized chitosan aerogel for gravity-driven oil/water separation. *Gels*, 7(2). Doi: [10.3390/gels7020066](https://doi.org/10.3390/gels7020066)